Radial oscillations of local density of states in carbon nanotubes

M. S. Ferreira,[1] T. G. Dargam,[2] R. B. Muniz,[2] and A. Latgé[2,*]
[1]*Department of Applied Physics and DIMES, Delft University of Technology, Lorentzweg 1, 2628 CJ Delft, The Netherlands*
[2]*Instituto de Física, Universidade Federal Fluminense, 24210-340, Niterói-RJ, Brazil*
(Received 16 October 2000; published 4 June 2001)

By performing an analytical study of the electronic structure of metallic carbon nanotubes, we show that the local density of states exhibits well-defined oscillations as a function of the nanotube radius. The periods of such oscillations are obtained from size quantization effects derived from folding up finite graphene sheets into tubular structures. A clear analogy with the de Haas–van Alphen effect in metals is established to explain the origin and features of such oscillations. Results of energy change calculations for impurity-doped carbon nanotubes also show the same type of oscillations.

DOI: 10.1103/PhysRevB.63.245111 PACS number(s): 71.20.Tx, 73.40.Ns

I. INTRODUCTION

Cylindrical molecules of carbon, known as carbon nanotubes (CN's), have been attracting considerable attention because of their especial physical properties. They are found in a wide variety of geometries with unique transport and electronic features. The possibility of being either metallic or semiconducting, depending merely on geometrical aspects of their structure,[1–3] is one of the most remarkable properties of CN's. The combination of interesting transport properties, mechanical strength, and flexibility makes CN's ideal candidates for building blocks of nanoscale electronic devices. In fact, several CN-based devices have been proposed, such as double quantum dots,[4] rectifying diodes,[5] and nanotube-based transistors.[6–8] A single-walled nanotube (SWNT) can be regarded as a single layer of graphite folded up into a cylinder. These tubular molecules are also found in multiple shells, where several cylinders are arranged in coaxial alignment, forming so-called multiwalled nanotubes (MWNT's). Although some interwall interaction is expected in these coaxial multitubule structures, the coupling between neighboring shells tends to be weak,[9] and multiwalled systems are sometimes described as a collection of independent single-wall CN's.

Motivated by the advances in growth techniques of CN junctions, where different CN are seamlessly fused together,[10] we recently addressed the question of how the local electronic properties of metallic-semiconducting CN heterostructures change as one moves along the tube from the metallic side to the semiconducting side of a junction.[11] Sufficiently far from the junction, the one-electron local density of states (LDOS) at the Fermi energy (E_F) vanishes exponentially on the semiconducting side, but oscillates around the bulk-limit value in the metallic side. Oscillations of the LDOS along the tube axis were experimentally observed in very short structures,[12] but they still need to be observed in long nanotubes. Commensurability between the periods and the lattice, together with intracell phase-shift effects, may be responsible for hiding the LDOS oscillations from experimental observations.

In this work we show that the LDOS of metallic SWNT's oscillates as a function of the nanotube radius. Although there have been several studies of the electronic structure of nanotubes, radial oscillations of the LDOS have not been reported. As a SWNT consists of a single layer of graphite folded up into a cylinder, the electronic structure of graphite is expected to be recovered for very large tube diameters. We show that this asymptotic limit is reached in an oscillatory way, and discuss the physical origin of such oscillations by analogy with the de Haas–van Alphen effect in metals. It is well known that some features of the de Haas–van Alphen oscillations, such as period and amplitude decay, are associated with wave vectors of the bulk Fermi surface of the corresponding metal. Likewise, a similar relation with the Fermi surface of the CN is used to explain the oscillations of the LDOS as a function of the tube diameter. The study of electronic properties of SWNT's as a function of the tube radius should reflect some characteristic features of their multiwalled counterparts. Such radial oscillations of the LDOS, in particular, may be observed by probing different shells of MWNT's.

There is experimental evidence that nanotubes may be doped by atoms attached to their walls during their growth,[13] and also by charge transfer from metal electrodes. Here we also treat the case of a substitutional impurity in single-walled and multiwalled metallic CN's. We first extend our approach to calculate the impurity binding energy as a function of the tube diameter in single-walled tubes. Our results exhibit a clear oscillatory behavior which is associated with the electronic structure of the nanotube host. We then repeat the calculations for a multiwalled NT structure, and show that the interwall interaction does not affect much the obtained results.

This paper is organized as follows: First, in Sec. II, we derive an analytical expression for the one-electron Green function of a semi-infinite armchair carbon nanotube, and show that it leads to a LDOS that may have an oscillatory behavior. In Sec. III we explicitly calculate the LDOS, and show that, in fact, it oscillates as a function of the tube diameter. Oscillation features such as periods and rates of decay are discussed, and a clear correspondence with the de Haas–van Alphen effect in metallic systems is established. In Sec. IV, we discuss the effect of oscillations on local electronic properties of MWNT's and impurity binding energies. Finally, in Sec. V, we draw our main conclusions.

II. SINGLE-PARTICLE GREEN FUNCTIONS

We are interested in studying the electronic properties of infinitely long CN's as a function of their radius. For the sake of simplicity, and with no loss of generality, we study achiral CN's. More specifically, we consider metallic armchair nanotubes, but our results and analysis can easily be extended to other geometries, including chiral metallic tubes. To investigate the LDOS's of SWNT's and MWNT's, it is convenient to treat the electronic structure in terms of single-particle Green functions, which have been previously used to study nanotube heterojunctions,[11,14] and the conductance of CN's with defects.[15] In those cases, due to the inhomogeneous nature of the systems considered, the so-called Green function matching method was used, where Green functions of different defect-free tubes were matched to represent composite tubes. The corresponding Green functions for the pure tubes were numerically calculated by recursive[16] or iterative[17] techniques.

Carbon nanotubes are fullerenelike structures, which can be regarded as graphene sheets wrapped up in cylindrical shape. The electronic structures of both graphene and CN's are well described by a single-band tight-binding model for the π orbitals, the only difference between them being the wave-vector quantization along the circumferential direction of the tubes. The one-dimensional energy dispersion for the armchair CN is given by

$$E_m^{\pm}(k_y) = \pm \gamma_0 \left[1 + 4\cos\left(\frac{m}{N_x}\pi\right)\cos\left(k_y\frac{a}{2}\right) + 4\cos^2\left(k_y\frac{a}{2}\right)\right]^{1/2},$$

where $a = 2.46$ Å, is the lattice parameter of graphene, and γ_0 is the hopping integral between nearest neighbors, hereafter used as our energy unit. N_x corresponds to the number of carbon sites in the CN unit cell, and $m = 1,2,\ldots,N_x$ labels the different bands. For such a simple band structure, it is possible to obtain the single-particle Green functions analytically.

The LDOS is given by the imaginary part of the diagonal Green function,

$$G(\omega) = \frac{1}{2N}\sum_{\mathbf{k}}\left[\frac{1}{\omega - E^+(\mathbf{k})} + \frac{1}{\omega + E^+(\mathbf{k})}\right], \tag{1}$$

where ω is the energy, N is the number of unit cells in the tube, and $\mathbf{k} = (k_x, k_y)$ is a wave vector in the two-dimensional graphene Brillouin zone. We recall that k_x assumes discrete values $k_{x,m} = (m/N_x)(\pi/a\sqrt{3})$, where m is an integer number labeling the wave-vector quantization along the circumferential direction. The sum over k_y may be replaced by an integral, and Eq. (1) can be rewritten as

$$G(\omega) = \frac{a}{4N_x\pi}\sum_m \int_{-\pi/a}^{\pi/a} dk_y \left[\frac{\omega}{\omega^2 - E_m^{+2}(k_y)}\right]. \tag{2}$$

We recall that N_x is directly associated with the tube diameter. For each value of k_x, we have a corresponding one-dimensional band structure. The integral above can be evaluated by extending k_y to the complex plane.[11] We change the integration contour from a straight line on the real axis to the boundaries of a semi-infinite rectangle in the upper half-plane whose base lies on the real axis between $-\pi/a$ and π/a. By determining the poles and their respective residues, we can evaluate the integral for each band index m. The poles, labeled $q_m^{\pm}$, are given by

$$\cos\left(q_m^{\pm}\frac{a}{2}\right) = -\frac{1}{2}\left\{\cos\left(\frac{m}{N_x}\frac{\pi}{2}\right) \pm \sqrt{\frac{\omega^2}{\gamma_0^2} - \sin^2\left(\frac{m}{N_x}\frac{\pi}{2}\right)}\right\}, \tag{3}$$

and the corresponding residues are

$$Res[q_m^{\pm}] = \frac{\omega}{2a\gamma_0^2}\left\{\cos\left(\frac{m}{N_x}\frac{\pi}{2}\right)\sin\left(q_m^{\pm}\frac{a}{2}\right) + \cos\left(q_m^{\pm}\frac{a}{2}\right)\sin\left(q_m^{\pm}\frac{a}{2}\right)\right\}^{-1}. \tag{4}$$

Equation (3) does not define the poles $q_m^{\pm}$ uniquely. By defining the cosine of $q_m^{\pm}$ but not its sine, the residue in Eq. (4) is free to assume two distinct values. The residue depends on the correct sign of $\sin[q_m^{\pm}(a/2)]$, which is obtained by imposing that the imaginary part of the retarded local Green functions must be negative. The expression for $G(\omega)$ then becomes

$$G(\omega) = \frac{i\omega}{N_x\gamma_0^2}\sum_{q_m^{\pm}}\left\{\cos\left(\frac{m}{N_x}\frac{\pi}{2}\right)\sin\left(q_m^{\pm}\frac{a}{2}\right) + \cos\left(q_m^{\pm}\frac{a}{2}\right)\sin\left(q_m^{\pm}\frac{a}{2}\right)\right\}^{-1}. \tag{5}$$

It is noteworthy that the poles $q_m^{\pm}$ depend upon both ω and N_x, as shown in Eq. (3). Each term of the summation corresponds to a band contribution to the single-particle Green function. Figure 1 shows the real and imaginary parts of the diagonal Green function of an armchair CN obtained from Eq. (5). One benefit of having such an analytical expression for the Green function is the fact that it allows a transparent analysis of the relationship between the electronic structure and the relevant parameters involved. Contrary to previous analytical treatments,[18,19] our approach makes no assumption about the energy bands being linear. Therefore, within a single-orbital approximation, it is valid in the entire energy-band range. Other effects, however, such as the σ-π hybridization, may limit our single-orbital treatment. One particular advantage of Eq. (5) is that it yields an explicit expression for the N_x dependence of the LDOS. We recall that, apart from a $1/N_x$ multiplying factor, all the other N_x-dependent terms appear inside trigonometric functions. As previously mentioned, the poles $q_m^{\pm}$ depend on N_x, and, as shown in Eq. (3), such a dependence is governed by similar elementary trigonometric functions. Therefore, Eq. (5)

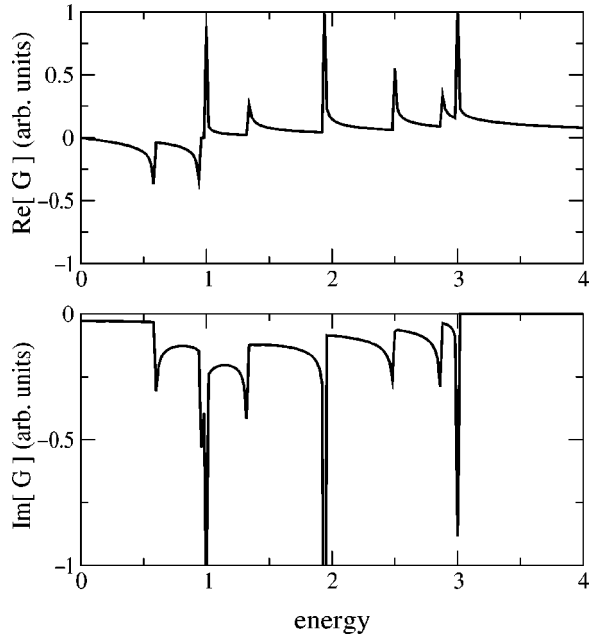

FIG. 1. Real (full line) and imaginary (dotted curve) parts of the diagonal Green function of a metallic armchair CN (5,5) obtained from Eq. (5). All energy values are in units of $\gamma_0 \approx 3$ eV.

explicitly shows that the diagonal Green functions, hence the LDOS, of infinitely long armchair CN's may oscillate as the tube diameter is increased.

III. RADIAL OSCILLATIONS OF THE LDOS

In Sec. II, we showed that the diameter dependence of the Green function is governed by trigonometric functions, which may lead to an oscillatory behavior of the LDOS as the tube radius is changed. Here we explicitly calculate the Green functions, and confirm the existence of such oscillations. Rather than plotting the LDOS along the entire energy band for different tubes, we plot it as a function of the tube radius for different energies. Four curves are displayed corresponding to $E=0$, 0.10, 0.15, and 0.30, respectively. Figure 2(a), associated with $E=0$, shows no oscillations, but a monotonically decaying behavior toward the asymptotic LDOS value of graphene. More precisely, the LDOS decays as $1/R$, where R is the tube radius.[20] However, for $E \neq 0$, clear oscillations become evident in the LDOS, as shown in Figs. 2(b), 2(c), and 2(d). Those oscillations have well-defined periods that decrease with increasing energy, for relatively small energy changes around $E=0$. All cases considered here show a $1/R$ overall decaying rate. One should note that the radius of an armchair CN is constrained by

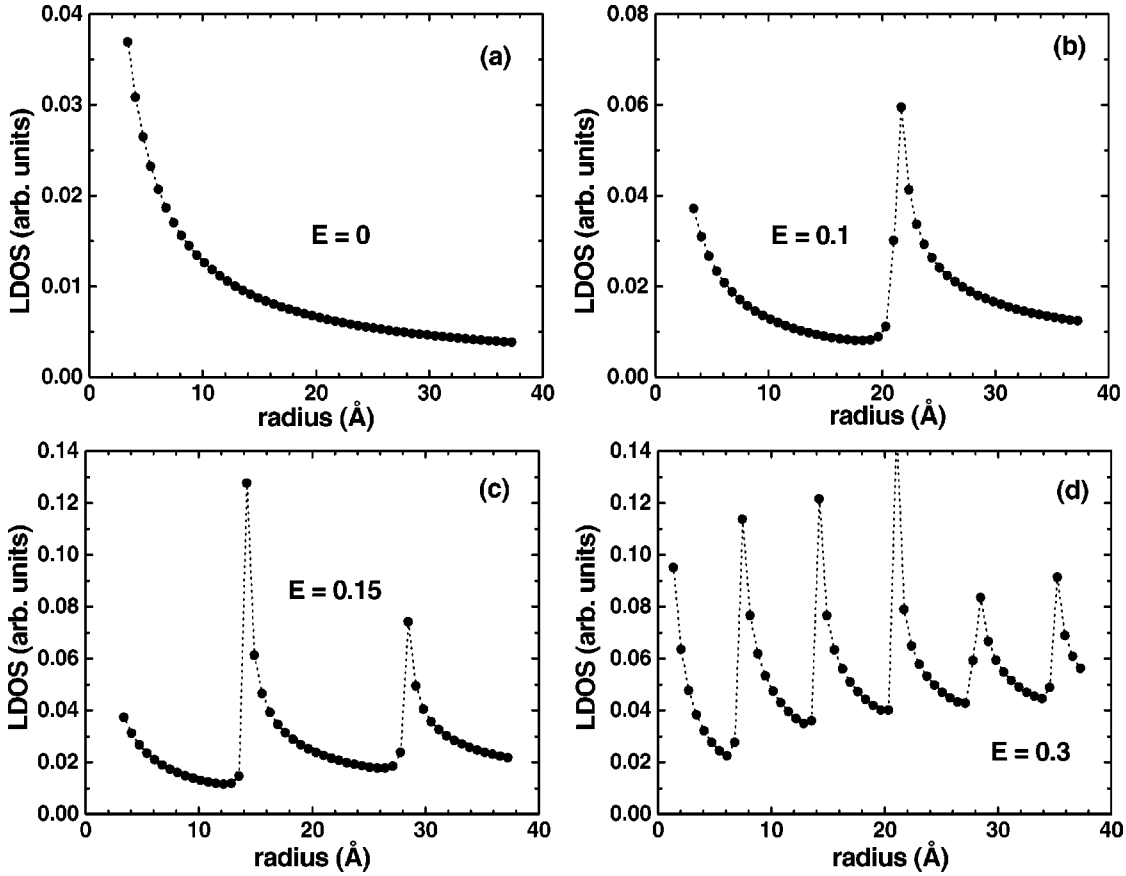

FIG. 2. Local density of states as a function of the tube radius for (a) $E=0$, (b) 0.10 , (c) 0.15, and (d) 0.30. The nanotube radius r is related to the integer n of an (n,n) armchair NT by $a\sqrt{3}n/(2\pi)$, a being the lattice parameter. All energy values are in units of $\gamma_0 \approx 3$ eV.

geometrical aspects of the hexagonal lattice and tube chirality. Thus it can only acquire a discrete set of values. The dashed lines shown in Fig. 2 serve as a guide for the eye, and the points represent the actual possible values of the tube diameters.

To understand the nature of the oscillations, we establish an analogy with the de Haas–van Alphen effect in metallic systems.[21] It is well known that several electronic properties depending on the density of states at E_F oscillate as a function of an applied magnetic field. Such oscillations are caused by magnetic-field-induced quantized levels periodically crossing the Fermi energy as the field strength is varied. The shape of the metallic Fermi surface determines the oscillation features, making the de Haas–van Alphen effect a useful tool to map out Fermi surfaces of several metals.[22]

The analogy between the radial oscillations of the LDOS in CN's with the de Haas–van Alphen effect is then clear. Instead of being caused by a magnetic field, the energy quantization in the nanotubes comes from the boundary conditions imposed on the graphene electronic structure, as a result of folding up the graphite sheet into a tubular structure. The wave-vector quantization along the circumferential direction is a size effect, and depends on the perimeter of the tube. By changing the tube diameter, the quantized levels move along the energy spectrum. Analogously to the de Haas–van Alphen effect, oscillations will occur as the quantized levels cross the Fermi energy. Figure 3(a) shows several contour plots of constant-energy lines in the two-dimensional hexagonal Brillouin zone of graphene. For $E=0$, the contour plot is a set of isolated points that coincide with the six vertices of the Brillouin zone. As the energy increases, they become small contours around those vertices, up to the point where the energy reaches the van Hove singularity of graphene at $E=1$. At this energy, the constant-energy plot becomes a collection of straight lines crossing the first Brillouin zone at the middle of their six edges, connecting the nearest M points. Further changes in energy lead to increasingly smaller circular contours approaching the center of the zone at the Γ point. Figure 3(b) shows the Brillouin zone for the armchair CN, for two different tube diameters and for two distinct values of energy E. For the sake of clarity, and to avoid a confusing figure with many quantized lines, we consider small diameters and well-separated energies only. The full vertical lines correspond to $N_x=2$, and the dashed ones are for $N_x=3$. The dashed and full lines coincide at the center and at the edge of the two-dimensional Brillouin zone, because those high-symmetry values of k_x are common to all diameters. Therefore, it is clear why the LDOS does not oscillate for $E=0$ in Fig. 2(a). The constant-energy plot in this case corresponds to six isolated points at the high-symmetry corners of the hexagonal two-dimensional Brillouin zone (2DBZ). Since we are dealing with metallic armchair CN's, there is only one quantized wave vector ($k_x=0$) that intersects the isolated points associated with $E=0$. As the diameter is increased, the density of lines in the Brillouin zone also increases, but no additional lines ever intersect the corners of the Brillouin zone. Therefore, no oscillations occur in this case, in agreement with previous calculations concerning the radial dependence of local electronic properties at $E_F=0$.[23] However, the distribution of constant-energy plots in the 2DBZ changes for $E\neq 0$, as illustrated in Fig. 3(b) by circular and triangular-shaped contours. The oscillations for each value of E_F, seen in Figs. 2(b)–2(d), come from the k_x-quantized levels intersecting the corresponding constant-energy contours, as the tube radius varies. This is illustrated in Fig. 3(b), where we show two energy plots selected from Fig. 3(a), together with the k_x-quantized lines. Clearly, by changing $N_x=2$ to $N_x=3$, the dashed lines approach both contours.

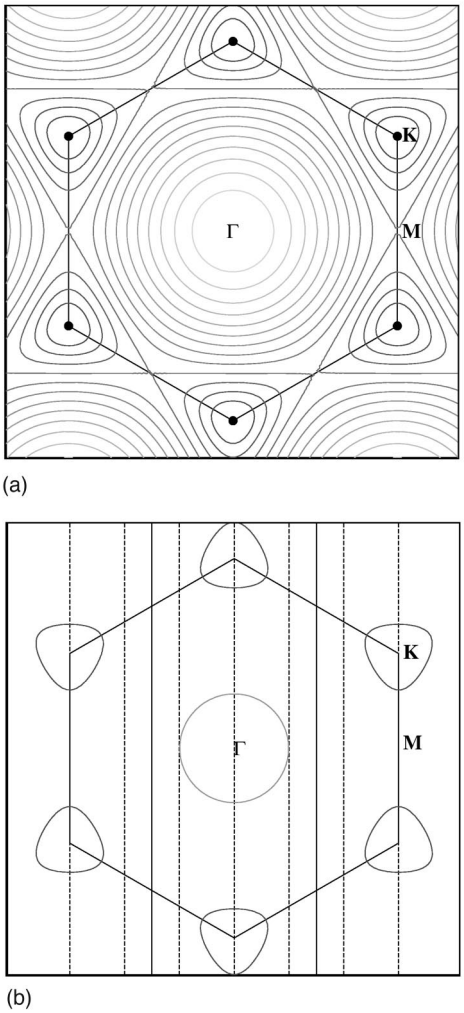

FIG. 3. (a) Contour plots for some constant-energy lines within the two-dimensional hexagonal Brillouin zone of graphene. (b) Brillouin zone for the armchair CN. Full vertical lines correspond to $N_x=2$, and the dashed lines to $N_x=3$. The circle close to the zone center and the triangular-shaped contours correspond to energies $E=0.6$ and 2.65, respectively, given in units of $\gamma_0\approx 3$ eV.

The intersections between the constant-energy plots and the size-quantized k_x lines may be determined by setting $\partial E(k_y)/\partial k_y=0$, where $E(k_y)$ is the one-dimensional energy dispersion for the armchair CN. This leads to $\cos(k_y a/2)=-(1/2)\cos(m\pi/N_x)$. Substituting such expression in $E(k_y)$, we see that the intersections occur when

$$N_x=\frac{m\pi}{\sin^{-1}(E_F/\gamma_0)}. \tag{6}$$

It follows that the LDOS at E_F, and properties that depend on it, will oscillate as a function of the CN radius, with a period $p=\Delta N_x a\sqrt{3}/(2\pi)$. The relation above is in perfect agreement with our numerical calculations, and has been verified for all cases considered.

IV. DOPED SINGLE-WALLED AND MULTIWALLED NANOTUBES

The study of impurity-related physical properties of semiconducting systems is very important, because transport and optical phenomena are strongly affected by the presence of impurities. Moreover, impurity segregation in metallic alloys and ultrathin films is also relevant from a technological point of view. In the nanotube structure, substitutional *p* and *n* doping with B and N atoms, respectively, was theoretically suggested[24] and experimentally accomplished. Impurity-screening properties are found to be completely dominated by the π bands,[25] and they are also sensitive both to the impurity position and to the tubular structure.

Here we show that the oscillatory behavior displayed by the LDOS as a function of the tube diameter is also present in the binding energy of a substitutional impurity placed on single-walled and multiwalled nanotubes. We highlight that such radial oscillations may induce absolute minima in the binding energy, leading to energetically favorable positions for the impurities. We suggest that modulation in the impurity concentration as a function of the tube radius may occur in multiwalled nanotubes.

We first concentrate on the case of doped single-walled nanotubes. The energy variation due to the insertion of a single substitutional impurity can be written in terms of the Green functions of the pure nanotubes via the Dyson equation $F=G+GV_0F=G+GTG$, where $T=V_0(1-GV_0)^{-1}$, F and G are the perturbed and unperturbed Green functions, respectively, and V_0 denotes the scattering potential associated with an isolated impurity at the site labeled 0. The total-energy variation $\Delta\epsilon$ due to the impurity is given by

$$\Delta\epsilon=-\frac{1}{\pi}\int_{-\infty}^{E_F}d\omega\,\mathrm{Im}\,\mathrm{Tr}\sum_j\,(F_{j,j}-G_{j,j}), \tag{7}$$

where *j* runs over the CN unit cells, and the trace is over the carbon sites in each unit cell. Therefore, by using cyclic properties of the trace, and integrating by parts, such an energy change may be rewritten as

$$\Delta\epsilon=-\frac{1}{\pi}\mathrm{Im}\left\{E_F\ln[1-G_{0,0}(E_F)V_0]-\int_{-\infty}^{E_F}d\omega\ln[1-G_{0,0}(\omega)V_0]\right\}, \tag{8}$$

where $G_{0,0}$ denotes the site-diagonal unperturbed Green function at the impurity site.

Since $G_{0,0}$ oscillates as a function of the CN radius, one expects an oscillatory behavior for $\Delta\epsilon$. It is noteworthy that the screening, and hence V_0, changes with the CN radius. In some cases, the potential V_0 may be determined by modeling the charge transfer due to the impurity. For metallic systems,

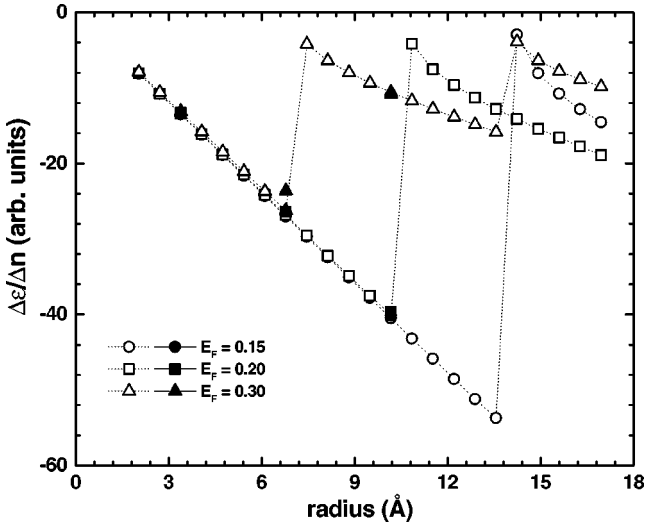

FIG. 4. Total-energy change as a function of the tube radius for different Fermi energies. Dotted lines are just to guide the eye, since the nanotube radius is a discrete quantity. Filled symbols correspond to the connected (5,5)-(10,10)-(15,15) MWNT's. All energy values are in units of $\gamma_0\approx 3$ eV.

V_0 is usually obtained by imposing either local or global charge neutrality. The latter provides a simple prescription, known as the Friedel sum rule, to determine V_0 in terms of the atomic number difference between the impurity and the host.[26] Here, rather than discussing specific impurities, we are interested in studying the general dependence of the impurity binding energy on the CN radius. It is then instructive to consider the weak-scattering limit, corresponding to $V_0 \ll 1$. In this case, Eq. (8) reduces to

$$\Delta\epsilon\approx V_0\{n_0-E_F\rho_0(E_F)\}, \tag{9}$$

where ρ_0 and n_0 are the unperturbed electronic LDOS and occupation number at the impurity site, respectively. Also, in the weak-scattering limit, according to the Friedel sum rule,

$$V_0\approx-\Delta n/\rho_0(E_F), \tag{10}$$

where Δn is the valence difference between the impurity and the host material. It follows from Eq. (9) that

$$\Delta\epsilon\approx\Delta n\left[E_F-\frac{n_0}{\rho_0(E_F)}\right]. \tag{11}$$

Due to the fact that ρ_0 oscillates as a function of the CN radius, it is clear that $\Delta\epsilon$ will also do so, and with the same periods as discussed in Sec. III. This is explicitly demonstrated in Fig. 4, where we show results of $\Delta\epsilon/\Delta n$ calculated as a function of the CN radius for different Fermi energies. The oscillations are evident, except for $E_F=0$ where they are not expected, as previously discussed.

V. EFFECTS OF INTERWALL INTERACTION IN MWNT'S

A multiwalled nanotube consists of a set of coaxial single-walled nanotubes, connected by weak interwall inter-

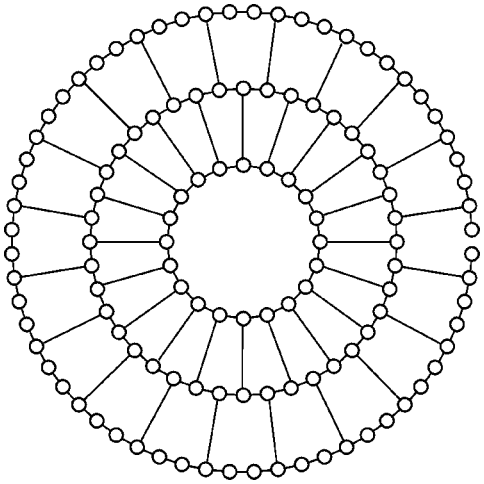

FIG. 5. Schematic representation of the adopted interwall connections between the (5,5)-(10,10)-(15,15) trilayered tube.

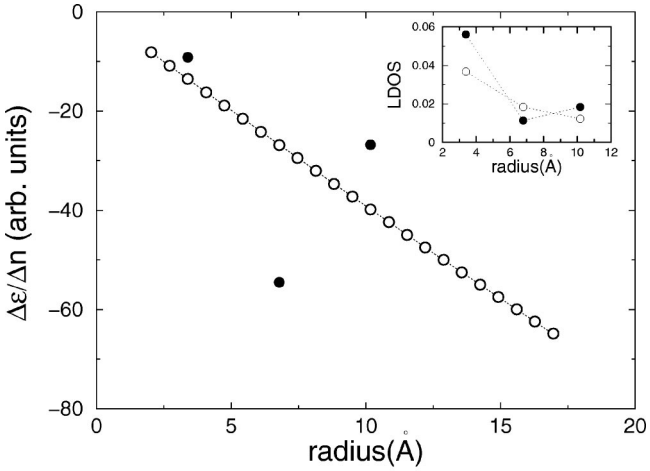

FIG. 6. Total-energy change as a function of the tube radius for $E_F=0$. Open and filled circles refer to single tubes and to the connected (5,5)-(10,10)-(15,15) MWNT's, respectively. The inset shows the corresponding averaged LDOS at $E_F=0$. All the energy values are in units of $\gamma_0 \approx 3$ eV.

actions. Within the tight-binding approximation we allow electrons to hop across adjacent tubes at some sites, with an effective intersite hopping integral γ. The interwall distance is roughly the same as the interlayer distance of graphite (≈ 0.34 nm), and $\gamma \approx \gamma_0/10$. Here we wish to investigate how this interwall interaction would affect the oscillatory features we have obtained. We consider a (5,5)-(10,10)-(15,15) multiwalled structure, radially connected as shown in Fig. 5. The unit cell of such a system comprises three interconnected rings, and contains a total of 120 carbon atoms. We have used a real-space renormalization technique to calculate the site-diagonal Green function, and the LDOS, at each atom along the structure.[11] Our results for the LDOS at E_F, and for the electronic occupation number, have been averaged over the inequivalent carbon sites situated on each ring. For most energies they do not differ much from those obtained with $\gamma=0$, corresponding to a set of isolated tubes. The same applies to the calculated values of $\Delta\epsilon$, as illustrated in Fig. 4 by filled symbols. For $E_F=0$, however, interwall interactions in armchair MW structures break the accidental degeneracy between the valence and conduction bands that takes place at $k=2\pi/3a$ in the one-dimensional Brillouin zone.[9] Consequently, the Fermi surface ceases to be a collection of just six isolated points coinciding with the vertices of the 2DBZ. Thus the comensurability between the period of oscillations and the lattice no longer exists, and an oscillatory behavior for the LDOS and $\Delta\epsilon$ emerges, as shown in Fig. 6.

Quantitatively, our results may depend upon the model used to describe the interwall interaction. Nevertheless, the radial oscillations reported here are present in MWCN's, and are likely to be observed in such structures.

VI. CONCLUSIONS

We have studied some local electronic properties of single-walled and multiwalled armchair CN's. We have shown that the LDOS oscillates as a function of the CN radius. The physical origin, periods, and other features of such oscillations are explained in terms of size quantizations due to the folding up of the CN's in the circumferential direction. A close analogy between the LDOS oscillations and the de Haas–van Alphen effect in metallic systems is established. We have calculated the binding energy of substitutional single impurities, and showed that they also oscillate as a function of the CN radius, with the same periods as those of the LDOS oscillations. Such an oscillatory behavior of $\Delta\epsilon$ suggests that a radial modulation of the impurity concentration may occur in MWNT's. The weak interwall interaction in MWNT's may have very little effect on our results. Thus, there is a very good chance for those oscillations to be observed in MWCN's. Actually, it is currently possible to control the structure of MWNT's, by peeling off the most external layers and removing part of their inner shells, and exposing tubes with different diameters.[27] Such an experimental setup may be very convenient to investigate some of our predictions. Multiple shell nanowires[28,29] are also good candidates for presenting the types of oscillations we have discussed.

ACKNOWLEDGMENTS

We would like to thank the Brazilian agencies CNPq, CAPES, and FAPERJ for partial financial support.

*Electronic address: latge@if.uff.br

[1] M.S. Dresselhaus, G. Dresselhaus, and R. Saito, Phys. Rev. B **45**, 6234 (1992); M.S. Dresselhaus, G. Dresselhaus, and P.C. Eklund, *Science of Fullerenes and Carbon Nanotubes* (Academic Press, New York, 1996); R. Saito, G. Dresselhaus, and M.S. Dresselhaus, *Physical Properties of Carbon Nanotubes* (Imperial College Press, London, 1998).

[2] S. Ijima, Nature (London) **354**, 56 (1991).

[3] J.W.G. Wildoer, L.C. Venema, A.G. Rinzler, R.E. Smalley, and C. Dekker, Nature (London) **391**, 59 (1998).

[4] J. Lefebvre, J.F. Lynch, M. Llaguno, M. Radosavljevic, and A.T. Johnson, Appl. Phys. Lett. **75**, 3014 (1999).
[5] Z. Yao, H.W.C. Postma, L. Balents, and C. Dekker, Nature (London) **402**, 273 (1999); R.D. Antonov and A.T. Johnson, Phys. Rev. Lett. **83**, 3274 (1999).
[6] S.J. Tans, M.H. Devoret, H. Dai, A. Thess, R.E. Smalley, L.J. Geerligs, and C. Dekker, Nature (London) **386**, 474 (1997).
[7] M. Bockrath, D.H. Cobden, P.L. McEuen, N.G. Chopra, A. Zettl, A. Thess, and R.E. Smalley, Science **275**, 1922 (1997).
[8] S.J. Tans, A.R.M. Verschueren, and C. Dekker, Nature (London) **393**, 49 (1998).
[9] R. Saito, G. Dresselhaus, and M.S. Dresselhaus, J. Appl. Phys. **73**, 494 (1993); M.S. Dresselhaus, G. Dresselhaus, and R. Saito, Phys. Rev. B **45**, 6234 (1992).
[10] C. Dekker, Nature (London) **402**, 273 (1999).
[11] M.S. Ferreira, T.G. Dargam, R.B. Muniz, and A. Latgé, Phys. Rev. B **62**, 16 040 (2000).
[12] L.C. Venema, J.W.G. Wildoer, H.L.J. Temminck Tuinstra, C. Dekker, A.G. Rinzler, and R.E. Smalley, Appl. Phys. Lett. **71**, 2629 (1997).
[13] R. Martel, T. Schmidt, H.R. Shea, T. Hertel, and Ph. Avouris, Appl. Phys. Lett. **73**, 2447 (1998).
[14] L. Chico, V.H. Crespi, L.X. Benedict, S.G. Louie, and M.L. Cohen, Phys. Rev. Lett. **76**, 971 (1996).
[15] L. Chico, L.X. Benedict, S.G. Louie, and M.L. Cohen, Phys. Rev. B **54**, 2600 (1996).
[16] J. Godfrin, J. Phys.: Condens. Matter **3**, 7843 (1991).
[17] M.P. Lopez Sancho, J.M. Lopez Sancho, and J. Rubio, J. Phys. F: Met. Phys. **14**, 1205 (1984); **15**, 851 (1985).
[18] J.-C. Charlier and Ph. Lambin, Phys. Rev. B **57**, R15 037 (1998).
[19] J.W. Mintmire and C.T. White, Phys. Rev. Lett. **81**, 2506 (1998).
[20] J.W. Mintmire, D.H. Robertson, and C.T. White, J. Phys. Chem. Solids **54**, 1835 (1993).
[21] D.M. Edwards, J. Mathon, R.B. Muniz, and S. Phan, Phys. Rev. Lett. **67**, 493 (1991).
[22] N.W. Ashcroft and N.D. Mermim, *Solid State Physics* (Holt, Rinehart and Wilson, New York, 1976).
[23] T. Kostyrko, M. Bartkowiak, and G.D. Mahan, Phys. Rev. B **59**, 3241 (1999).
[24] J. Yel Yi and J. Bernholc, Phys. Rev. B **47**, 1708 (1993).
[25] M.F. Lin and D.S. Chuu, Phys. Rev. B **56**, 4996 (1997).
[26] J. Friedel, Adv. Phys. **3**, 446 (1954).
[27] John Cumings and A. Zettl, Science **289**, 602 (2000).
[28] G. Bilalbegovic, Phys. Rev. B **58**, 15 412 (1998).
[29] Y.R. Hacohen, E. Grunbaum, R. Tenne, J. Sloan, and J.L. Hutchinson, Nature (London) **395**, 336 (1998).